Research Square

Preprints are preliminary reports that have not undergone peer review.
They should not be considered conclusive, used to inform clinical practice,
or referenced by the media as validated information.

Molecular sex identification revealed a high proportion of sex-reversed individuals in natural populations of Mauremys mutica

Siqi Liu
Anhui Normal University
Yuxin Dai
Anhui Normal University
Tingting Chen
Anhui Normal University
Zhiyuan Yang
Anhui Normal University
Ziyao Meng
Anhui Normal University
Jianjun Liu
Anhui Normal University
Liuwang Nie
lwnie@mail.ahnu.edu.cn

Anhui Normal University

Research Article

Keywords: Mauremys mutica, transcriptomics, karyotype, sex reversal

Posted Date: June 19th, 2026

DOI: https://doi.org/10.21203/rs.3.rs-9972436/v1

License: This work is licensed under a Creative Commons Attribution 4.0 International License.
Read Full License

Additional Declarations: No competing interests reported.

Abstract

Turtles exhibit both genetic sex determination (GSD), which encompasses XY and ZW systems, and temperature-dependent sex determination (TSD). Although the Asian yellow pond turtle (*Mauremys mutica*) has been confirmed to possess an XY genetic system along with temperature effects, it currently lacks Y-chromosome-linked molecular markers. In this study, we integrated transcriptomic subtraction, genomic alignment, and cytogenetic analyses to isolate a male-specific Y-linked marker in *M. mutica*, which can reliably distinguish XX and XY genotypes in both hatchlings and adults via a 223-bp PCR product. Using this marker, we found that under extreme temperatures, the offspring included individuals with XX males and XY females, confirming temperature-induced sex reversal. Moreover, we detected a high frequency of sex reversal in natural populations of *M. mutica*, with XX males and XY females together comprising 33.6% of sampled adults. This provides the first genetic evidence of naturally occurring sex reversal in a freshwater turtle. The high frequency of sex reversal likely reflects that the Y chromosome has not yet acquired a dominant role in initiating male development. Our findings confirm the coexistence of GSD and TSD in *M. mutica* and establish a practical, non-invasive tool for genotypic sex identification.

1. Introduction

Sex determination in vertebrates is governed by diverse mechanisms that integrate genetic architecture with developmental cues to direct gonadal differentiation. The classic dichotomy contrasts genetic sex determination (GSD), where sex chromosomes dictate fate, with environmental sex determination (ESD), notably temperature-dependent sex determination (TSD) in reptiles and fishes (Bull 1983). However, these pathways are not mutually exclusive. Compelling evidence shows that GSD and TSD can coexist and interact, with thermal cues potentially overriding genetic signals to cause sex reversal—the development of a phenotypic sex opposite to the genotypic sex (Sarre et al., 2011; Holleley et al., 2015; Li et al., 2022; Whiteley et al., 2022; Lu et al., 2025). This interaction reveals a remarkable plasticity in vertebrate sex-determining systems (Ruiz-García et al., 2021; Zhang et al., 2025).

Sex chromosome systems themselves evolve along a continuum. The prevailing model of sex chromosome evolution proposes that both XY and ZW systems originate from a pair of autosomes following the emergence of a master sex-determining gene (MSDG), after which recombination is progressively suppressed around the sex-determining locus (Zhu et al., 2025). However, many non-model taxa possess younger, homomorphic sex chromosomes where the sex-determining region is limited and the Y or W chromosome retains much of its ancestral, autosomal-like state (Gamble et al., 2017; Jeffries et al., 2018; El Taher et al., 2021; Huang et al., 2023). In such young systems, the sex-determining gene's control is often less dominant, making them susceptible to being overridden by environmental factors such as temperature, thereby facilitating sex reversal (Holleley et al., 2015; Ruiz-García et al., 2021; Kitano et al., 2024).

Turtles provide an exceptional model system to investigate this interplay. The group exhibits both TSD and GSD, with XY and ZW systems having evolved independently multiple times (Valenzuela *et al.*, 2011; Bista *et al.*, 2020). While TSD is widespread and considered ancestral, GSD has been confirmed in specific lineages, such as some Pleurodiran families (e.g., Chelidae) and Cryptodiran families (e.g., Trionychidae) (Ewert *et al.*, 1991; Valenzuela *et al.*, 2011; Weber et al., 2020; Thépot 2021). Cytogenetic studies reveal a spectrum of sex chromosome differentiation in turtles, from homomorphic to highly heteromorphic states (Montiel et al., 2016). Despite this diversity, research into turtle sex determination has been severely limited by the lack of sex-linked molecular markers. Such limitations are especially acute in determining genotypic sex for most species, detecting natural sex reversal, and assessing its broader ecological and evolutionary significance.

The Asian yellow pond turtle (*Mauremys mutica*), a critically endangered freshwater speciesb, epitomizes this knowledge gap and presents a compelling case study. Initially classified as a TSD species, recent chromosomal-scale genomic analyses revealed a differentiated XY sex chromosome system, providing the first genomic evidence for the coexistence of GSD and TSD in a turtle species (Liu et al., 2025). This discovery positions *M. mutica* as a critical species for understanding how genetic and environmental pathways interact in turtles. However, the absence of a practical, Y-linked molecular marker has rendered key questions unanswerable: Does temperature-induced sex reversal occur? If so, how frequently does it happen in the natural populations? Current reliance on labor-intensive karyotyping for genotypic sexing is untenable for population-level studies.

To address this gap, we developed and validated a Y-linked molecular marker for *M. mutica*. We then used this marker to test for temperature-associated sex reversal under controlled incubation and to assess whether genotype–phenotype discordance also occurs in natural individuals. This study provides both a practical tool for genotypic sex identification and new evidence for sex reversal in *M. mutica*.

2. Results

2.1 Hatching success and sex ratios at different incubation temperatures

Incubation temperature significantly affected embryonic development, hatching success and phenotypic sex ratios in *M. mutica*. Incubation duration decreased significantly with increasing temperature. Hatching success remained high at both 26 ℃ (male-producing temperature, MPT) and 28 ℃ (97.5% and 95%, respectively), but declined markedly under 32 ℃ (female-producing temperature, FPT) conditions to 72.5%. Additionally, two hatchlings from the FPT group exhibited partial carapace defects, corresponding to a malformation rate of 6.4% (Table 1).

Table 1
Effects of incubation temperature on incubation period, survival rate, malformation rate, and Phenotypic sex ratio.

Incubation Temperature (℃)	Incubation Period (days)	Survival Rate (%)	Malformation Rate (%)	Phenotypic Sex Ratio (M: F)
26℃	93.23 ± 1.84	97.5	0	39:0
28℃	72.66 ± 3.34	95	0	17:21
32℃	61.97 ± 1.94	72.5	6.4	0:29
Note: Data are presented as mean ± standard deviation for incubation period.				

After one year of rearing, the gonads of *M. mutica* were fully developed, allowing sex determination through histological examination. The gonad-mesonephros complexes (GMCs) of individuals incubated at different temperatures were collected, and gonadal morphology was observed and photographed under a stereomicroscope. The results are shown in Fig. 1. Individuals incubated at 28 ℃ displayed elongated, slender, thread-like gonads in females (Fig. 1A) and short, thick, cylindrical gonads in males (Fig. 1B). All juveniles in the MPT group were male, and all from the FPT group were female.

Karyotype analysis was performed on 10 female and 10 male juvenile *M. mutica* that had been incubated at a constant temperature of 28 ℃ and reared for one year. The results showed that females had a diploid chromosome number of 2n = 52 with an XX sex chromosome constitution (Fig. 1C), whereas males also had 2n = 52 but exhibited a pair of clearly heteromorphic sex chromosomes (XY) (Fig. 1D). The overall karyotype pattern was 9 + 15 + 12 with an overall karyotype formula of 9 large, 15 medium, and 12 small chromosome pairs. These patterns are consistent with previous reports in this species (Du et al., 2010). Complete concordance between genotypic and phenotypic sex was observed at 28 ℃, where every XX individual (n = 10) exhibited female development and every XY individual (n = 10) exhibited male development, providing no evidence of sex reversal under this constant temperature.

2.2 Isolation and Validation of a Y-linked Marker

The presence of a Y chromosome was investigated using RNA-seq datasets from liver, heart, and gonadal tissues of one male and one female *M. mutica* with concordant phenotypic and karyotypic sex (Supplementary Table S1). A female-restricted transcriptome was first assembled and subsequently used as a reference to screen male-specific sequences. Assembly of the combined female RNA-seq datasets yielded 303,928 transcripts with a contig N50 of 1,724 bp. K-mer analysis using unmapped male RNA-seq reads in combination with female RNA-seq data identified 10,964,670 male-specific (Y) k-mers. Reads containing these Y-mers were extracted from the male RNA-seq dataset and assembled into a male-restricted transcriptome, generating 185,261 transcripts with a contig N50 of 699 bp (Table 2). Applying stringent filtering criteria, no reads mapped in females and a minimum depth of four reads in males, resulted in the identification of 56 candidate Y-linked transcripts longer than 400 nt

(Supplementary Table S2). This filtering strategy ensured the absence of female-derived reads while minimizing false-positive assignments in males.

Table 2
Statistics of transcriptome assembly and K-mers of female and male

Female Assembly	
Total transcripts	303,928
Contig N50 (bp)	1,724
Average contig (bp)	780.49
GC (%)	46.68
Y-mers	
Number of male k-mers	37,706,682
Number of female k-mers	41,985,486
Numbers of unique Y-mers	10,964,670
Male Assembly	
Total transcripts	185,261
Contig N50 (bp)	699
Average contig (bp)	559.82
GC (%)	47.78

To identify a robust Y-linked diagnostic marker, the 56 candidate male-specific transcripts were screened by PCR using genomic DNA from individuals with concordant phenotypic and karyotypic sex. Among these candidates, only TRINITY_DN56537_c2_g4_i1 (Mm-Y) consistently produced a male-specific amplification product. A diagnostic 223-bp fragment was detected exclusively in males, whereas the mitochondrial *COX1* positive control amplicon (1046 bp) was present in both sexes (Fig. 1E).

2.3 Genomic localization and structural characterization of a Y-linked marker

BLAST analysis of the candidate Y-linked transcript against the *M. mutica* reference genome showed that the full 706-bp sequence mapped to a single major genomic locus located at approximately 5.38 Mb on scaffold CM064395.1 (Fig. 2A, D). No additional high-confidence full-length matches were detected elsewhere in the genome, indicating that this transcript is associated with a principal diagnostic Y-linked locus. Structural analysis divided the transcript into three segments (1-225 bp, 226–427 bp, and 428–706 bp), each displaying distinct genomic alignment patterns (Fig. 2D). The 1-225 bp region exhibited

high sequence similarity to repetitive elements distributed across multiple chromosomes, supporting its annotation as a transposable element–derived fragment (Fig. 2B). In contrast, the downstream regions showed specific association with CM064395.1. The 226–427 bp segment aligned as a unique single-copy sequence, whereas the 428–706 bp segment produced multiple high-identity matches within the same genomic locus, consistent with local tandem duplication events (Fig. 2D). Further genomic inspection confirmed that the entire Y-linked marker resides within an approximately 5.38 Mb interval on CM064395.1 and lacks detectable homologous regions elsewhere in the genome (Fig. 2A, D). Divergence time estimation based on synonymous substitution rates suggested that the duplication event underlying the repeated 428–706 bp module occurred approximately 52.4 million years ago (Mya) (Fig. 2C). To ensure diagnostic specificity, PCR primers were deliberately designed to span the 226–706 bp region, thereby excluding the transposable element-containing 5' segment. This design minimizes the risk of cross-amplification from autosomal copies of repetitive elements and ensures specificity to the Y-linked haplotype. Together, these results establish the 706-bp transcript as a robust Y-linked diagnostic marker for identifying Y-chromosome presence in *M. mutica*.

2.4 Detection of incubation temperature-induced sex reversal using the Mm-Y marker

Phenotypic sex in hatchlings from the MPT (26 ℃) and FPT (32 ℃) groups was initially assigned on the basis of gonadal morphology, using the same morphological criteria as those applied to the 28 ℃ group. The primary objective of this experiment was to qualitatively determine whether temperature-induced sex reversal occurs in *M. mutica*, rather than to estimate its exact frequency within each incubation group. Therefore, we randomly selected 8 of the 29 phenotypic females from the FPT group and 8 of the 39 phenotypic males from the MPT group for further analysis. Individuals from these subsets were subjected to PCR analysis using the Mm-Y marker, and only those showing discordance between phenotypic sex and PCR results were further examined by immunofluorescence and karyotype analysis. Sex ratio analysis based on gonadal phenotype showed a clear temperature-dependent pattern: nearly all hatchlings developed as phenotypic males at 26 ℃ and as phenotypic females at 32 ℃ (Table 1), consistent with TSD-Ia type sex determination (Zhu et al., 2006).

In the FPT subset, PCR detected the Y-specific band in two of eight phenotypic females (Fig. 3A). Immunofluorescence analysis of these discordant individuals showed thickened cortical regions in the gonads, with no detectable DMRT1 signal, consistent with female phenotypic differentiation (Fig. 3B). However, karyotype analysis revealed a 2n = 52 karyotype with an XY sex chromosome constitution with a typical heteromorphic sex chromosome pair (Fig. 3D). Conversely, in the MPT subset, four of eight phenotypic males lacked the Y-specific band (Fig. 3A). Immunofluorescence analysis showed that these discordant individuals possessed a thin cortex and a loosely organized medulla, with strong nuclear DMRT1 signals in the developing seminiferous cords, indicating male phenotypic differentiation (Fig. 3C). Nevertheless, karyotype analysis showed a 2n = 52 karyotype with an XX sex chromosome constitution without heteromorphic sex chromosomes (Fig. 3E).

These results demonstrate the presence of sex-reversed individuals under both FPT and MPT incubation: genetic males (XY) developing as phenotypic females, and genetic females (XX) developing as phenotypic males. These individuals were designated as XY sex-reversed females (XY^f) and XX sex-reversed males (XX^m). Accordingly, PCR results in these individuals were inconsistent with their gonadal phenotypes.

2.5 Molecular sex identification in a natural population

Non-invasive DNA extraction and molecular sexing were performed on 125 adult *M. mutica* individuals collected from the southern Anhui and Lu'an regions (Fig. 4A, B) to evaluate the occurrence of sex reversal under natural conditions. Genetic sex was determined using the Mm-Y marker. Among the 81 phenotypic females, 14 tested positive for the Y-specific band (sex reversal frequency of 17.3%). Among the 44 phenotypic males, 28 tested negative for the Y-specific band (sex reversal frequency of 63.7%). Overall, sex-reversed individuals accounted for 33.6% of the sampled wild population (42 out of 125 individuals) (Fig. 4C).

Table 3
Field sampling site information and sex composition of *M. mutica* in Anhui Province

Sampling Site	Latitude and Longitude	Number of Females	Number of Males
Jinzhai County, Lu'an City	116°00'24.58"E, 31°36'58.03"N	15	9
Xihe Village, Dahuaping Town, Huoshan County, Lu'an City	116°16'22.32"E, 31°14'12.67"N	16	8
Foziling Scenic Area, Huoshan County, Lu'an City	116°16'22.32"E, 31°20'8.16"N	11	8
Tianlaozhuang, Sungang Township, Yeji District, Lu'an City	116°0'41.11"E, 31°51'32.24"N	8	5
Huoqiu County, Lu'an City	115°55'14.02"E, 32°12'36.86"N	6	5
Xuzhen Town, Nanling County, Wuhu City	118°26'15.19"E, 31°3'6.02"N	15	4
Xikou Town, Xuanzhou District, Xuancheng City	118°42'34.18"E, 30°38'54.74"N	10	5

3. Discussion

3.1 Development and validation of a Y-linked molecular sex marker

The development of the Y-linked molecular marker Mm-Y provides a practical tool for genotypic sex identification in *M. mutica*. Unlike sexing methods based on gonadal histology or cytogenetic analysis, this marker requires only a small amount of tissue-derived DNA and therefore offers a less invasive and more efficient approach for genotypic sexing across developmental stages. This is particularly valuable in hatchlings and juveniles, in which external sexual dimorphism is absent and gonadal morphology cannot be reliably assessed without dissection. Because Mm-Y can be detected by a simple PCR assay, it also provides a feasible method for screening larger sample sets for genotypic sex in both laboratory experiments and wild populations.

Our previous analysis of the X chromosome of *M. mutica* showed that approximately 95.9% of its sequence consists of repetitive elements and contains only a few annotated genes(Liu et al., 2025). The Y-linked transcript identified by the Mm-Y marker is also repetitive in nature and shares homology with repeat families that are enriched across multiple chromosomes; no recognizable functional gene was identified. These features indicate that, despite a heteromorphic (XY) karyotype, the sex chromosomes remain at a relatively early stage of differentiation, and the Y chromosome is dominated by repetitive elements rather than protein-coding genes. Despite its repetitive nature, the Mm-Y locus can be specifically targeted to distinguish XX from XY individuals. It showed consistent male-specific amplification in individuals with concordant phenotypic and karyotypic sex, and its diagnostic performance was further corroborated by immunofluorescence and karyotype analyses in discordant individuals. Because the identification of sex-reversed individuals may be confounded by morphological variation, developmental asynchrony, or marker misclassification, we adopted an integrated approach that combines PCR, gonadal phenotype, and karyotype evidence to validate discordant cases. This multi-method framework increases confidence in sex-reversal assignment and provides a stronger basis than reliance on any single technique alone. Recent work in birds has likewise stressed that genotype–phenotype discordance detected by PCR-based sexing should be evaluated using additional lines of evidence wherever possible (Whiteley et al., 2021; Potvin et al., 2026).

Two limitations of the Mm-Y marker should be noted. First, it cannot distinguish XY from YY genotypes. Second, the transcriptomic subtraction approach used for its discovery was based on a limited number of reference individuals and is not designed to comprehensively catalog all Y-linked transcripts. Despite these limitations, Mm-Y provides a reliable tool for genotypic sexing and opens new opportunities for investigating sex-ratio dynamics, sex-reversal frequency, and the interaction between genotype and incubation temperature in both natural and experimental populations. It may also serve as a useful molecular tool for conservation monitoring, particularly in species where climate-associated shifts in sex ratio are of concern.

3.2 Evidence for temperature-associated sex reversal under controlled incubation

Using the Mm-Y marker, we detected clear genotype–phenotype discordance among hatchlings incubated under both MPT and FPT, demonstrating that temperature-associated sex reversal occurs in

M. mutica. Under FPT conditions, a subset of phenotypic females carried the Y-specific marker and exhibited an XY karyotype, whereas under MPT conditions, several phenotypic males lacked the Y-specific marker and were cytogenetically confirmed as XX individuals. Immunofluorescence further showed that these individuals displayed gonadal differentiation patterns consistent with their phenotypic, rather than genotypic, sex. Taken together, these results provide direct evidence that incubation temperature can override the expected phenotypic outcome associated with chromosomal sex in this species. These findings support the view that sex determination in M. mutica reflects an interaction between genetic and thermal cues rather than a strictly canalized chromosomal system alone (Quinn et al., 2007; Schwanz et al., 2020; Lockley *et al.*, 2021). Comparable complexity has been reported in other reptiles in which chromosomal sex determination coexists with environmental sensitivity, such as the viviparous skink *Carinascincus ocellatus*, where sex reversal occurs within an XY system but does not fully explain all climate-mediated sex-ratio variation (Sarre et al., 2004; Quinn et al., 2007; Hill et al., 2022).

3.3 Analysis of potential causes of sex reversal in a natural population

Among 125 wild adult *M. mutica* individuals collected from the Lu'an region, a total of 42 genotype–phenotype discordant individuals were detected, representing an overall proportion of 33.6%. From the phenotypic perspective, 14 out of 81 phenotypic females carried the Y-specific marker (XY females, 17.3%), and 28 out of 44 phenotypic males lacked the Y-specific marker (XX males, 63.6%), indicating that genotype–phenotype discordance was particularly prominent among phenotypic males. From the genotypic perspective, 14 of the 30 Y-positive individuals were female (46.7%), and 28 of the 95 Y-negative individuals were male (29.5%). These results suggest that both XX and XY genotypes in the wild exhibit high environmental sensitivity, and the XY genotype does not confer an absolutely stable male fate.The high proportion of sex reversal in the wild population is likely driven primarily by the heterogeneity of natural nest temperatures. *M. mutica* exhibits TSD with female bias at high temperatures and male bias at low temperatures. Natural nests in the Lu'an region, which has a subtropical monsoon climate, are subject to substantial microhabitat variation in factors such as vegetation shading, soil moisture, and oviposition depth. During the thermosensitive period, some embryos may therefore experience temperatures that override their genetic sex signals, producing XX males or XY females. Similar temperature-induced sex reversal has been documented in the three-lined skink (*Bassiana duperreyi*), where cool natural nests induce XX male development, with reversal frequencies reaching 28.6% (Quinn et al., 2009; Dissanayake et al., 2021).

The sex chromosome system of *M. mutica* likely remains at an early stage of differentiation, as evidenced by the repeat-rich, gene-poor Y chromosome described above. Such poorly differentiated systems are expected to be more susceptible to environmental override. Notably, the 33.6% sex-reversal frequency we observed in the wild is substantially higher than that reported in other reptiles with confirmed wild-caught sex reversal, such as *Bassiana duperreyi* and *Pogona vitticeps* (Holleley et al.,

2015; Dissanayake et al., 2021; Whiteley et al., 2021). Such a high frequency suggests that the sexual development outcome of *M. mutica* is highly sensitive to thermal disturbance in the environment.

4. Materials and Methods

4.1 Gradient temperature incubation of fertilized eggs

Fertilized eggs of *M. mutica* were obtained from the Anhui Provincial Key Laboratory of Biodiversity Conservation and Ecological Security in the Yangtze River Basin, College of Life Science, Anhui Normal University, China. Eggs were incubated at three constant temperatures: 26 ℃ (male-producing temperature, MPT), 28 ℃ (intermediate incubation temperature), and 32 ℃ (female-producing temperature, FPT). A total of 120 eggs were used, with 40 fertilized eggs randomly assigned to each temperature treatment group.

To control for potential maternal effects, eggs were collected from 40 adult females, with three eggs sampled from each female and evenly distributed across the three temperature groups. Incubation duration, hatching mortality, and malformation rates were recorded for each temperature group. Following hatching, all surviving juveniles were reared under standardized aquaculture conditions for one year, allowing for clear gonadal differentiation prior to sex identification in subsequent experiments. Sex was first assessed based on gonadal morphology.

All experimental procedures were approved by the Animal Protection and Utilization Committee of Anhui Normal University (Approval No. #20221020) and were conducted in accordance with institutional guidelines for the care and use of animals.

4.2 Gradient temperature incubation of fertilized eggs Sex identification by gonadal dissection

To determine the sex of hatchlings from each temperature treatment group, gonadal morphology was examined by dissection. After one year of rearing, individuals were euthanized, and the gonad–mesonephros complex was exposed under a stereomicroscope (Leica M205A) by carefully incising along both sides of the carapace–plastron junction and removing the overlying visceral tissue. Sex was assigned based on gonadal morphology and size.

4.3 Cell culture and metaphase chromosome preparation for cytogenetic analyses

Primary cardiomyocyte cultures were established from the hearts of one-year-old M. mutica individuals, including ten phenotypically sexed females and ten males from the 28 ℃ group, as well as four individuals from the 26 ℃ group and two individuals from the 32 ℃ group showing genotype-phenotype sex inconsistency. Heart tissues were digested with trypsin–EDTA, and cells were maintained in DMEM supplemented with 15% fetal bovine serum, 2 mM L-glutamine, and 1% antibiotic–antimycotic at 29 ℃

under 5% CO_2. For chromosome preparation, cultured cells were treated with colcemid, subjected to hypotonic treatment in 0.075 M KCl, and fixed in ethanol–acetic acid before Giemsa staining and karyotype analysis (Liu et al., 2025).

4.4 Sample collection and RNA extraction

From the 28 ℃ incubation group, one male and one female confirmed by karyotype (Section 4.3) to have concordant phenotypic and genotypic sex were selected for transcriptome analysis. These two individuals were used for transcriptome analysis. Total RNA was extracted from heart, liver, and gonadal tissues using TRIzol reagent (Invitrogen, CA, USA) following the manufacturer's protocol. RNA quantity and integrity were assessed using an Agilent 2100 Bioanalyzer with the RNA 1000 Nano LabChip Kit, and only samples with RIN values > 7.0 were used for RNA-seq library construction.

4.5 RNA-seq Library Preparation and Sequencing

Poly(A) + RNA was purified from total RNA using poly-T oligo-attached magnetic beads with two rounds of purification. Purified mRNA was fragmented using divalent cations at elevated temperature and reverse-transcribed to generate cDNA libraries following the Illumina mRNA-seq Sample Preparation Kit protocol. Paired-end libraries with an average insert size of 300 ± 50 bp were sequenced on an Illumina HiSeq 4000 platform (LC Sciences, USA).

Raw sequencing data have been deposited in the NCBI Sequence Read Archive (SRA) under accession numbers SRR13283007–SRR13283012.

4.6 Assembly and identification of Y-linked transcripts

A transcriptome subtraction strategy was employed to identify Y-linked transcripts. First, female RNA-seq reads from heart, liver, and gonad were assembled de novo using Trinity v2.1.1 (Grabherr et al., 2011) to generate a female reference transcriptome. Second, male RNA-seq reads from the corresponding tissues were aligned to this female transcriptome using Bowtie v1.3.1 with the parameters -v 0 --best (Langmead et al., 2009), and unmapped reads were retained as putatively male-specific reads. To further reduce false-positive candidates, residual male-derived k-mers shared with female sequence data were removed from the unmapped read set, and the remaining male-enriched reads were re-assembled de novo using Trinity. Only transcripts longer than 400 nt were retained for downstream analyses in order to facilitate reliable primer design and marker validation. These candidate transcripts were aligned to the *M. mutica* reference genome (GCA_032357905.1) using BLASTn (Madden 2013) with an E-value cutoff of 1e-5. Transcripts showing high-confidence genomic matches (99–100% identity) were retained for further evaluation. To assess sex specificity, male and female RNA-seq reads, together with genomic DNA resequencing reads from concordant male and female individuals, were mapped back to the candidate transcripts using Bowtie (-v 0 --best). Mean read coverage was calculated using BEDTools v2.30.0 (Quinlan *et al.*, 2010). Transcripts showing coverage greater than 4× in males and zero coverage in females were retained as high-confidence candidate Y-linked transcripts. This filtering yielded 56 candidate transcripts, which were subsequently taken forward for PCR-based

validation. Candidate transcripts were prioritized for screening on the basis of male-specific transcriptomic subtraction, sequence completeness, primer designability, and the absence of confident support in female-derived data.

4.7 Specificity validation of Y-linked marker

Genomic DNA was extracted from muscle tissues using the phenol–chloroform method. Initially, to validate candidate Y-linked transcripts and identify a reliable Y-linked marker, we focused on the 28 ℃ incubation group, in which phenotypic sex had previously been confirmed to be concordant with karyotypic sex. Phenotypic males and phenotypic females from the 28 ℃ group (n = 10 each) served as reference controls. Multiple primer pairs were designed for PCR screening of the candidate Y-linked transcripts. Among these, a Y-linked molecular marker, designated Mm-Y, was identified from the transcript TRINITY_DN56537_c2_g4_i1. A specific primer pair (forward: 5’-ATGCAGCTACTGCCTCTCTTC-3’; reverse: 5’-AACTGCAGCTGCCTAGAAAGT-3’) was designed to amplify a 223-bp diagnostic fragment. PCR amplification was performed under the following conditions: 35 cycles with an annealing temperature of 58 ℃ and an extension time of 30 s. As an internal control, a 1046-bp fragment of the mitochondrial *COX1* gene was amplified in parallel using the primer pair forward 5’-GTCATCGTTACAGCCCATGC-3’ and reverse 5’-AGTACCCAGTGAAGAGCGGG-3’. Subsequently, to evaluate the amplification pattern of the Mm-Y marker under different temperature conditions, PCR validation was performed on random subsets of 8 phenotypic males from the 26 ℃ (MPT) group and 8 phenotypic females from the 32 ℃ (FPT) group.

4.8 Gonadal immunofluorescence staining for sex identification

Individuals with discordant results between PCR-based genotyping and gonadal morphology, specifically Y-positive phenotypic females and Y-negative phenotypic males, were selected for further analysis. Gonadal tissues were fixed in 4% paraformaldehyde, paraffin-embedded, and sectioned at 5 μm. Sections were deparaffinized, rehydrated, subjected to citrate-buffer antigen retrieval, and blocked with 5% BSA. Samples were incubated with primary antibodies overnight at 4°C, followed by fluorescent secondary antibodies for 1 h at room temperature. Nuclei were counterstained with DAPI, and images were acquired using a fluorescence microscope. Primary antibodies: rabbit anti-DMRT1 (1:200; Zhongding Biological Technology Co., Ltd., China) and mouse anti-β-catenin (1:200; ab22656; Abcam, Cambridge, MA, USA). Secondary antibodies: Fluoro 488–conjugated goat anti-rabbit IgG (BA1045-488; 1:500; Boster) and Fluoro 550–conjugated goat anti-mouse IgG (BA1133; 1:500; Boster).

4.9 Bioinformatic analysis of the Y-linked marker

Genomic localization of the Y-linked marker was determined by BLASTn searches against the *M. mutica* genome (GCA_032357905.1) using an E-value cutoff of 1e-20. The corresponding genomic sequences were then extracted using SeqKit v2.10.1 (Shen et al., 2016), aligned with MAFFT (Katoh *et al.*, 2013), and analyzed in MEGA X (Kumar et al., 2018) to calculate genetic distances. Divergence time was estimated

using the formula T = D / 2μ, where μ = 8.44e-10 (Ren et al., 2022). All analyses and visualizations were performed in R.

4.10 Non-invasive sampling of natural adults and DNA extraction

A total of 125 adult individuals of the natural population of *M. mutica* were collected from southern Anhui and the Lu'an region, Anhui Province, China (Table 3 and Fig. 4A), including 81 phenotypic females and 44 phenotypic males. All samples were obtained non-invasively during routine field surveys. The specific procedure was as follows: After capturing a *M. mutica* individual in the field, the turtle was rinsed with distilled water. A sterile swab was then used to scrub the limb pits, head and neck, tail, and other body surfaces more than 20 times to collect epithelial cells, without causing any injury to the animal. After sampling, all individuals were immediately released back to their original capture sites. The swabs were placed into 1.5 mL sterile EP tubes pre-filled with 500 μL of sample preservation solution and kept in a 4°C icebox. Genomic DNA was extracted using the TIANamp Swab DNA Kit (DP322; TIANGEN, China) according to the manufacturer's instructions, for subsequent molecular sex identification and validation using Mm-Y.

Declarations

Acknowledgments

The authors thank the reviewers and editors for their valuable comments on the manuscript.

Funding

This research was supported by the National Natural Science Foundation of China (NSFC, No. 32270553 to L.N. and NSFC,No. 32300409 to J.L.), and the China Postdoctoral Science Foundation

(2025M771917 to J.L.).

References

1. Bista B. and Valenzuela N. Turtle insights into the evolution of the reptilian karyotype and the genomic architecture of sex determination. Genes, 2020, 11(4): 416.https://doi.org/10.3390/genes11040416.
2. Bull J.J. 1983. Evolution of sex determining mechanisms. Benjamin/Cumings.
3. Dissanayake D.S., Holleley C.E. and Georges A. Effects of natural nest temperatures on sex reversal and sex ratios in an Australian alpine skink. Scientific Reports, 2021, 11(1): 20093.https://doi.org/10.1038/s41598-021-99702-1.
4. Du W.-G., Wang L. and Shen J.-W. Optimal temperatures for egg incubation in two Geoemydid turtles: Ocadia sinensis and Mauremys mutica. Aquaculture, 2010, 305(1-4): 138–

142.https://doi.org/10.1016/j.aquaculture.2010.03.032.

5. El Taher A., Ronco F., Matschiner M., Salzburger W. and Böhne A. Dynamics of sex chromosome evolution in a rapid radiation of cichlid fishes. Science Advances, 2021, 7(36): eabe8215.https://doi.org/10.1126/sciadv.abe8215.
6. Ewert M.A. and Nelson C.E. Sex determination in turtles: diverse patterns and some possible adaptive values. Copeia, 1991: 50–69.https://doi.org/10.2307/1446248.
7. Gamble T., Castoe T.A., Nielsen S.V., Banks J.L., Card D.C., Schield D.R., Schuett G.W. and Booth W. The discovery of XY sex chromosomes in a Boa and Python. Current Biology, 2017, 27(14): 2148–2153.https://doi.org/10.1016/j.cub.2017.06.010.
8. Grabherr M.G., Haas B.J., Yassour M., Levin J.Z., Thompson D.A., Amit I., Adiconis X., Fan L., Raychowdhury R. and Zeng Q. Trinity: reconstructing a full-length transcriptome without a genome from RNA-Seq data. Nature Biotechnology, 2011, 29(7): 644.https://doi.org/10.1038/nbt.1883.
9. Hill P., While G.M., Burridge C.P., Ezaz T., Munch K.L., McVarish M. and Wapstra E. Sex reversal explains some, but not all, climate-mediated sex ratio variation within a viviparous reptile. Proceedings of the Royal Society B: Biological Sciences, 2022, 289(1976): 20220689–20220689.https://doi.org/10.1098/rspb.2022.0689.
10. Holleley C.E., O'Meally D., Sarre S.D., Marshall Graves J.A., Ezaz T., Matsubara K., Azad B., Zhang X. and Georges A. Sex reversal triggers the rapid transition from genetic to temperature-dependent sex. Nature, 2015, 523(7558): 79–82.https://doi.org/10.1038/nature14574.
11. Huang Z., Xu L., Cai C., Zhou Y., Liu J., Xu Z., Zhu Z., Kang W., Cen W. and Pei S. Three amphioxus reference genomes reveal gene and chromosome evolution of chordates. Proceedings of the National Academy of Sciences, 2023, 120(10): e2201504120.https://doi.org/10.1073/pnas.2201504120.
12. Jeffries D.L., Lavanchy G., Sermier R., Sredl M.J., Miura I., Borzée A., Barrow L.N., Canestrelli D., Crochet P.-A. and Dufresnes C. A rapid rate of sex-chromosome turnover and non-random transitions in true frogs. Nature communications, 2018, 9(1): 4088.https://doi.org/10.1038/s41467-018-06517-2.
13. Katoh K. and Standley D.M. MAFFT multiple sequence alignment software version 7: improvements in performance and usability. Molecular Biology and Evolution, 2013, 30(4): 772–780.https://doi.org/10.1093/molbev/mst010.
14. Kitano J., Ansai S., Takehana Y. and Yamamoto Y. Diversity and convergence of sex-determination mechanisms in teleost fish. Annual Review of Animal Biosciences, 2024, 12(1): 233–259.https://doi.org/10.1146/annurev-animal-021122-113935.
15. Kumar S., Stecher G., Li M., Knyaz C. and Tamura K. MEGA X: molecular evolutionary genetics analysis across computing platforms. Molecular Biology and Evolution, 2018, 35(6): 1547–1549.https://doi.org/10.1093/molbev/msy09.
16. Langmead B., Trapnell C., Pop M. and Salzberg S.L. Ultrafast and memory-efficient alignment of short DNA sequences to the human genome. Genome Biology, 2009, 10(3):

R25.https://doi.org/10.1186/gb-2009-10-3-r25.

17. Li S., Xu Z., Luo L., Ping J., Zhou H., Xie L. and Zhang Y. Latitudinal variation in the pattern of temperature-dependent sex determination in the Japanese gecko, Gekko japonicus. Animals, 2022, 12(8): 942.https://doi.org/10.3390/ani12080942.
18. Liu J., Liu S., Dong J., Tang M., Li T., Li J., Bu X., Xia X., Zhou H. and Nie L. Discovery of XY Sex Chromosomes in Mauremys mutica Provides Insights Into the Role of KDM6B Gene in Coexistence of Temperature-Dependent and Genetic Sex Determination. Molecular Ecology, 2025, 34(7): e17710.https://doi.org/10.1111/mec.17710.
19. Lockley E.C. and Eizaguirre C. Effects of global warming on species with temperature-dependent sex determination: Bridging the gap between empirical research and management. Evolutionary Applications, 2021, 14(10): 2361–2377.https://doi.org/10.1111/eva.13226.
20. Lu J., Huang S., Wei S., Cheng J., Li W., Fei Y., Yang J., Hu R., Huang S. and Zhai W. Heat inducible nuclear translocation of Kdm6bb drives temperature dependent sex reversal in Nile tilapia. PLOS Genetics, 2025, 21(4): e1011664.https://doi.org/10.1371/journal.pgen.1011664.
21. Madden T. (2013). The BLAST sequence analysis tool. The NCBI handbook. 2: 425–436.
22. Montiel E.E., Badenhorst D., Lee L.S., Literman R., Trifonov V. and Valenzuela N. Cytogenetic insights into the evolution of chromosomes and sex determination reveal striking homology of turtle sex chromosomes to amphibian autosomes. Cytogenetic and Genome Research, 2016, 148(4): 292–304.https://doi.org/10.1159/000447478.
23. Potvin D.A., Conroy G.G., Jelocnik M., Kasimov V., Gillett A., Portas T., Hill A. and Hall C.A. Invited reply: Rates of avian sex reversal: a response to Balogh et al. Biology Letters, 2026, 22(3).https://doi.org/10.1098/rsbl.2025.0741.
24. Quinlan A.R. and Hall I.M. BEDTools: a flexible suite of utilities for comparing genomic features. Bioinformatics, 2010, 26(6): 841–842.https://doi.org/10.1093/bioinformatics/btq033.
25. Quinn A.E., Georges A., Sarre S.D., Guarino F., Ezaz T. and Graves J.A.M. Temperature sex reversal implies sex gene dosage in a reptile. Science, 2007, 316(5823): 411–411.https://doi.org/10.1126/science.1135925.
26. Quinn A.E., Radder R.S., Sarre S.D., Georges A., Ezaz T. and Shine R. Isolation and development of a molecular sex marker for Bassiana duperreyi, a lizard with XX/XY sex chromosomes and temperature-induced sex reversal. Molecular Genetics and Genomics, 2009, 281(6): 665–672.https://doi.org/10.1007/s00438-009-0437-7.
27. Ren Y., Zhang Q., Yan X., Hou D., Huang H., Li C., Rao D. and Li Y. Genomic insights into the evolution of the critically endangered soft-shelled turtle Rafetus swinhoei. Molecular Ecology Resources, 2022, 22(5): 1972–1985.https://doi.org/10.1111/1755-0998.13596.
28. Ruiz-García A., Roco Á.S. and Bullejos M. Sex differentiation in amphibians: effect of temperature and its influence on sex reversal. Sexual Development, 2021, 15(1-3): 157–167.https://doi.org/10.1159/000515220.

29. Sarre S.D., Georges A. and Quinn A. The ends of a continuum: genetic and temperature-dependent sex determination in reptiles. Bioessays, 2004, 26(6): 639–645.https://doi.org/10.1002/bies.20050.
30. Sarre S.D., Ezaz T. and Georges A. Transitions between sex-determining systems in reptiles and amphibians. Annual Review of Genomics and Human Genetics, 2011, 12(1): 391–406.https://doi.org/10.1146/annurev-genom-082410-101518.
31. Schwanz L.E., Georges A., Holleley C.E. and Sarre S.D. Climate change, sex reversal and lability of sex-determining systems. Journal of Evolutionary Biology, 2020, 33(3): 270–281.https://doi.org/10.1111/jeb.13587.
32. Shen W., Le S., Li Y. and Hu F. SeqKit: a cross-platform and ultrafast toolkit for FASTA/Q file manipulation. PlOS One, 2016, 11(10): e0163962.https://doi.org/10.1371/journal.pone.0163962.
33. Thépot D. Sex chromosomes and master sex-determining genes in turtles and other reptiles. Genes, 2021, 12(11): 1822–1822.https://doi.org/10.3390/genes12111822.
34. Valenzuela N. and Adams D.C. Chromosome number and sex determination coevolve in turtles. Evolution, 2011, 65(6): 1808–1813.https://doi.org/10.1111/j.1558-5646.2011.01258.x.
35. Weber C., Zhou Y., Lee J.G., Looger L.L., Qian G., Ge C. and Capel B. Temperature-dependent sex determination is mediated by pSTAT3 repression of Kdm6b. Science, 2020, 368(6488): 303–306.https://doi.org/10.1126/science.aaz4165.
36. Whiteley S.L., Castelli M.A., Dissanayake D.S., Holleley C.E. and Georges A. Temperature-induced sex reversal in reptiles: prevalence, discovery, and evolutionary implications. Sexual Development, 2021, 15(1-3): 148–156.https://doi.org/10.1159/000515687.
37. Whiteley S.L., Wagner S., Holleley C.E., Deveson I.W., Marshall Graves J.A. and Georges A. Truncated jarid2 and kdm6b transcripts are associated with temperature-induced sex reversal during development in a dragon lizard. Science Advances, 2022, 8(16): eabk0275.https://doi.org/10.1126/sciadv.abk0275.
38. Zhang Y., Luo T. and Sun Y. A temperature-induced sex reversal mechanism in ricefield eels. Water Biology and Security, 2025: 100360.https://doi.org/10.1016/j.watbs.2025.100360.
39. Zhu X., Chen Y., Wei C., Liu Y. and Gui J. Temperature effects on sex determination in yellow pond turtle (Mauremys mutica Cantor). Acta Ecologica Sinica, 2006, 26(2): 620–625
40. Zhu Z., Younas L. and Zhou Q. Evolution and regulation of animal sex chromosomes. Nature Reviews Genetics, 2025, 26(1): 59–74.https://doi.org/10.1038/s41576-024-00757-3.

Figures

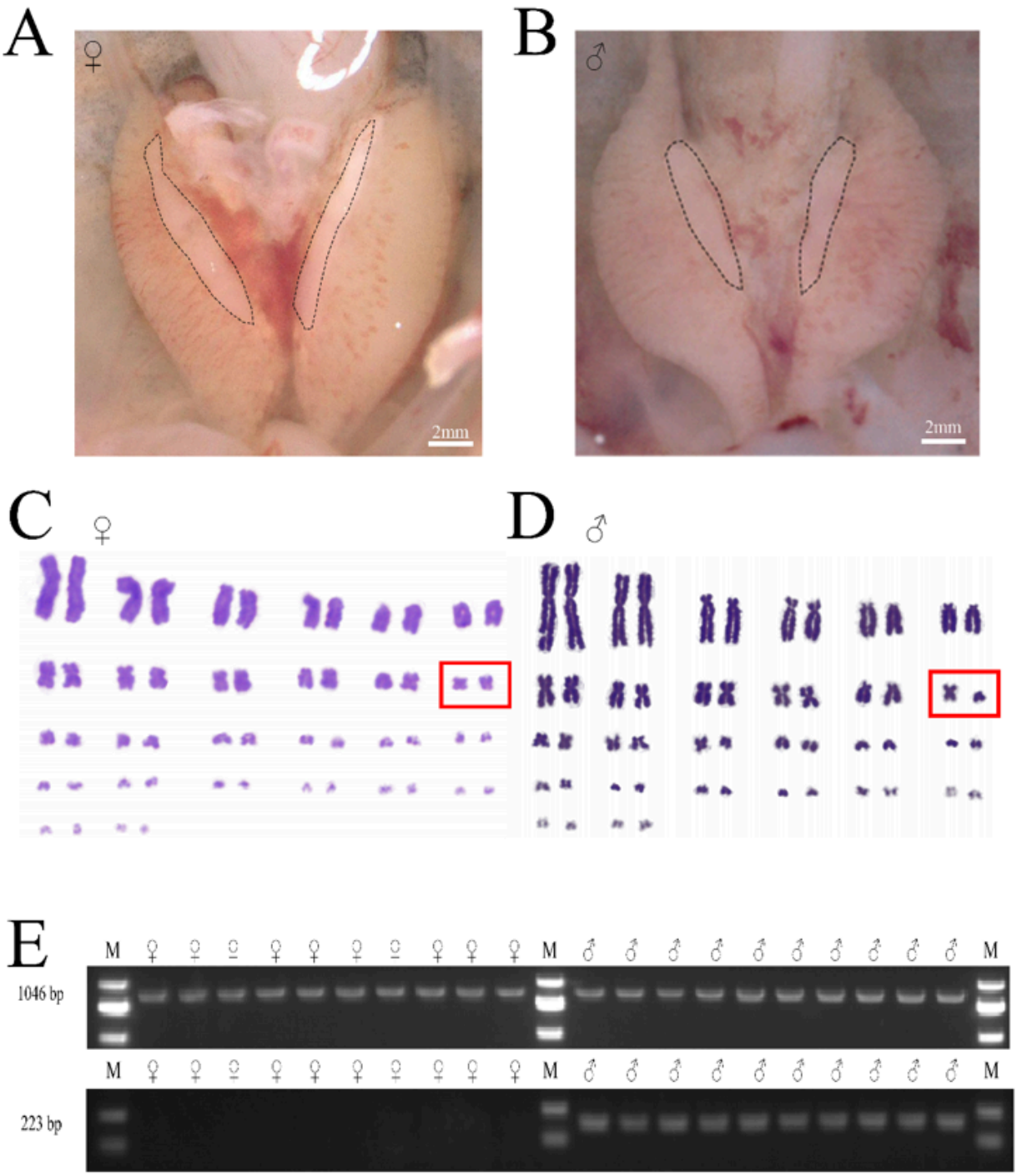


Figure 1

Gonadal morphology, karyotype, and PCR validation of the Y-linked marker in *M. mutica*.

(A) Female gonads from hatchlings incubated at 28 °C, showing elongated and slender morphology. (B) Male gonads from hatchlings incubated at 28 °C, showing short and thick morphology. Dashed outlines indicate the positions of the gonads. Scale bars = 2 mm. (C) Karyotype of a phenotypic female from the

28 °C group, showing a chromosomal complement of 2n = 52, XX. (D) Karyotype of a phenotypic male from the 28 °C group, showing a chromosomal complement of 2n = 52, XY. Red boxes indicate the sex chromosome pair. (E) PCR validation of the Y-linked molecular marker Mm-Y. The 223-bp diagnostic fragment was detected exclusively in males, whereas the mitochondrial *COX1*control fragment (1046 bp) was amplified in both females and males.

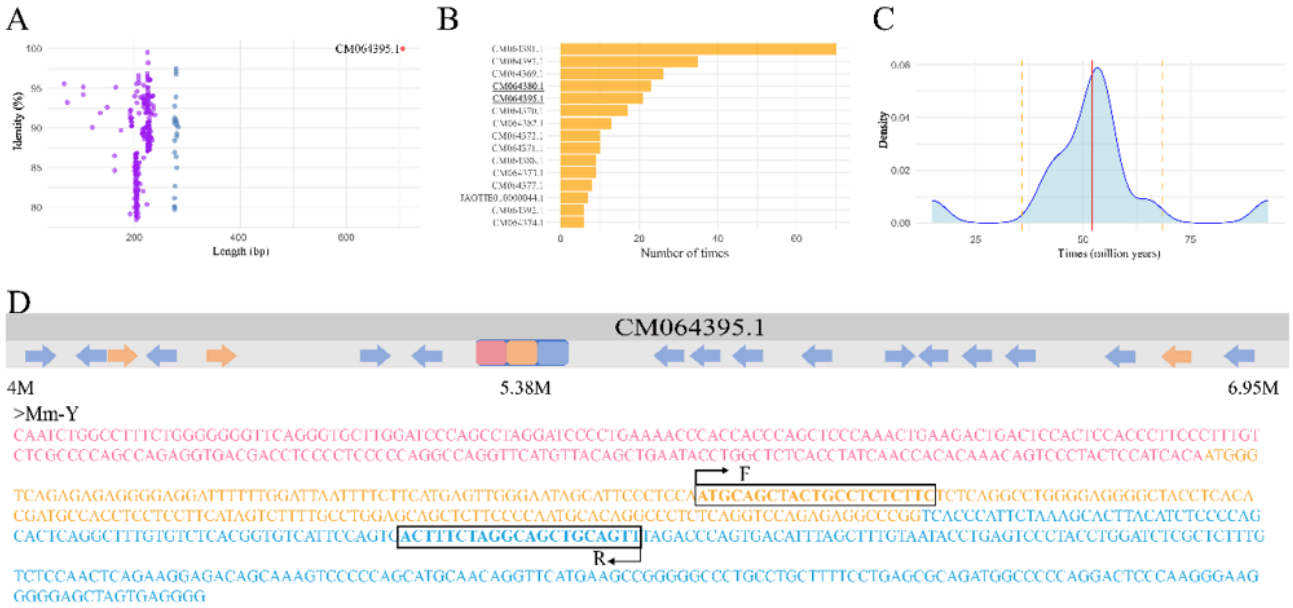


Figure 2

Genomic localization and structural features of the Y-linked molecular marker in *M. mutica*.

(A) Summary of BLAST alignments between the marker and the reference genome. Whole-transcript BLAST mapping indicates that the 706-bp sequence can be partitioned into three discrete alignment segments, each exhibiting a distinct genome-wide hit distribution pattern. (B) Distribution of BLAST hit counts across chromosomes/scaffolds, indicating that a repeat-associated portion of the marker generates matches on multiple scaffolds, whereas CM064395.1 represents the key target scaffold (highlighted in bold). (C) Density distribution of divergence-time estimates for the internal repeated module; the red vertical line indicates the point estimate and dashed lines denote the confidence interval. (D) Schematic of the marker locus on CM064395.1 (approximately 5.38 Mb) and dissection of marker architecture into three segments. The 5' segment shows repeat/transposable-element–like matches, whereas downstream segments display scaffold-specific alignment patterns including local tandem duplication. PCR primers (F/R) were designed to span the downstream scaffold-specific region to maximize Y-haplotype specificity and minimize non-specific amplification from repetitive sequences.

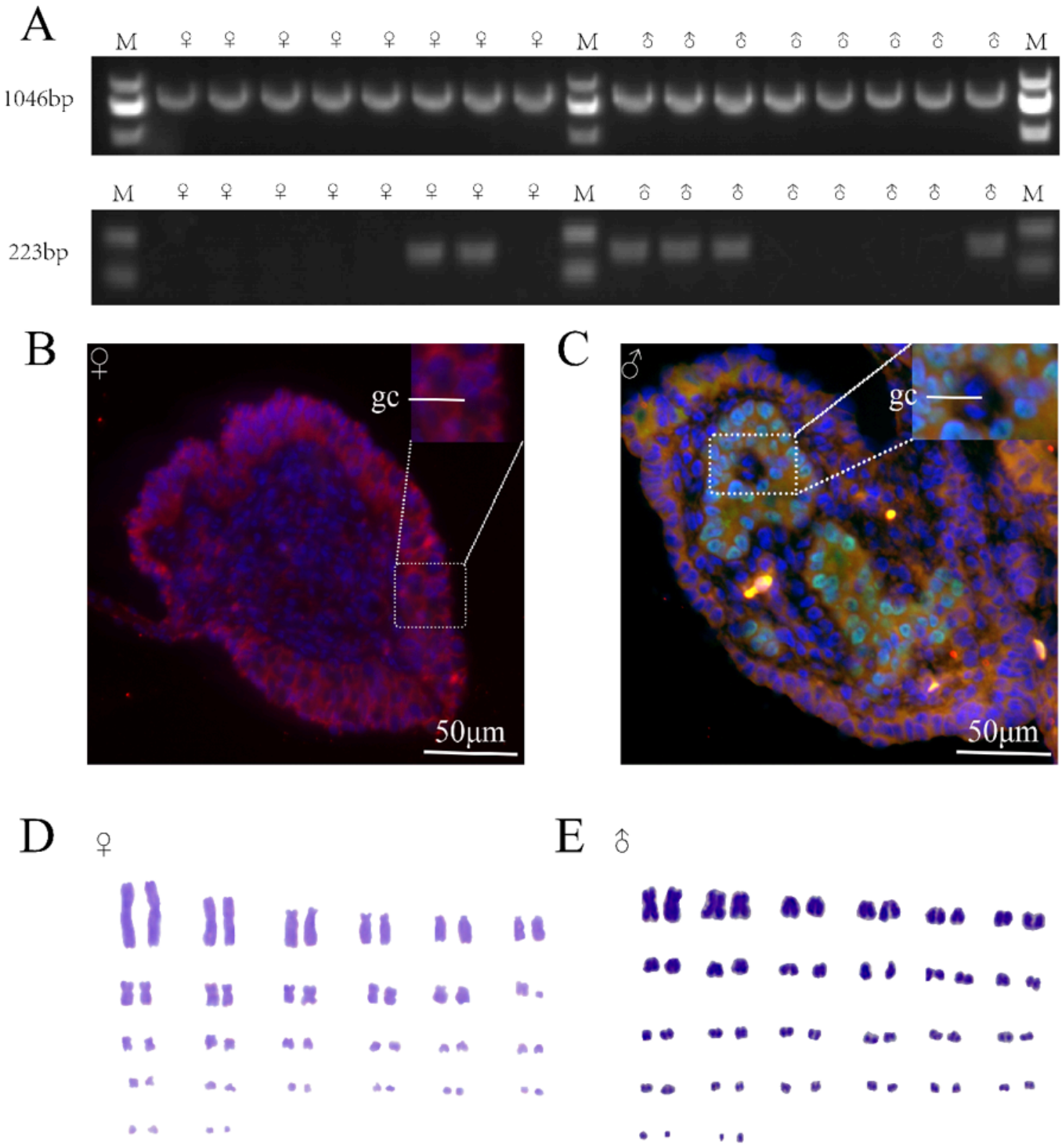


Figure 3

Identification of sex-reversed individuals in *M. mutica* by PCR, immunofluorescence, and karyotype analyses.

(A) PCR detection of the Y-linked marker Mm-Y in phenotypic females and phenotypic males incubated under FPT and MPT conditions, respectively. The upper panel shows amplification of the mitochondrial *COX1* control fragment (1046 bp), and the lower panel shows the diagnostic Mm-Y fragment (223 bp).

Two phenotypic females carried the Y-specific band, whereas four phenotypic males lacked the Y-specific band, indicating genotype–phenotype discordance. (B) Immunofluorescence image of a phenotypic female gonad, showing a thickened cortical region and no detectable DMRT1 signal, consistent with female gonadal differentiation. (C) Immunofluorescence image of a phenotypic male gonad, showing a thin cortex and a loosely organized medulla, with strong nuclear DMRT1 signals in the developing testicular cords, consistent with male gonadal differentiation. Insets show enlarged views of the boxed regions. (D) Karyotype of the phenotypic female shown in (B), revealing a 2n = 52, XY chromosomal complement. (E) Karyotype of the phenotypic male shown in (C), revealing a 2n = 52, XX chromosomal complement. Nuclei were counterstained with DAPI (blue). Scale bars = 50 μm. gc, germ cell.

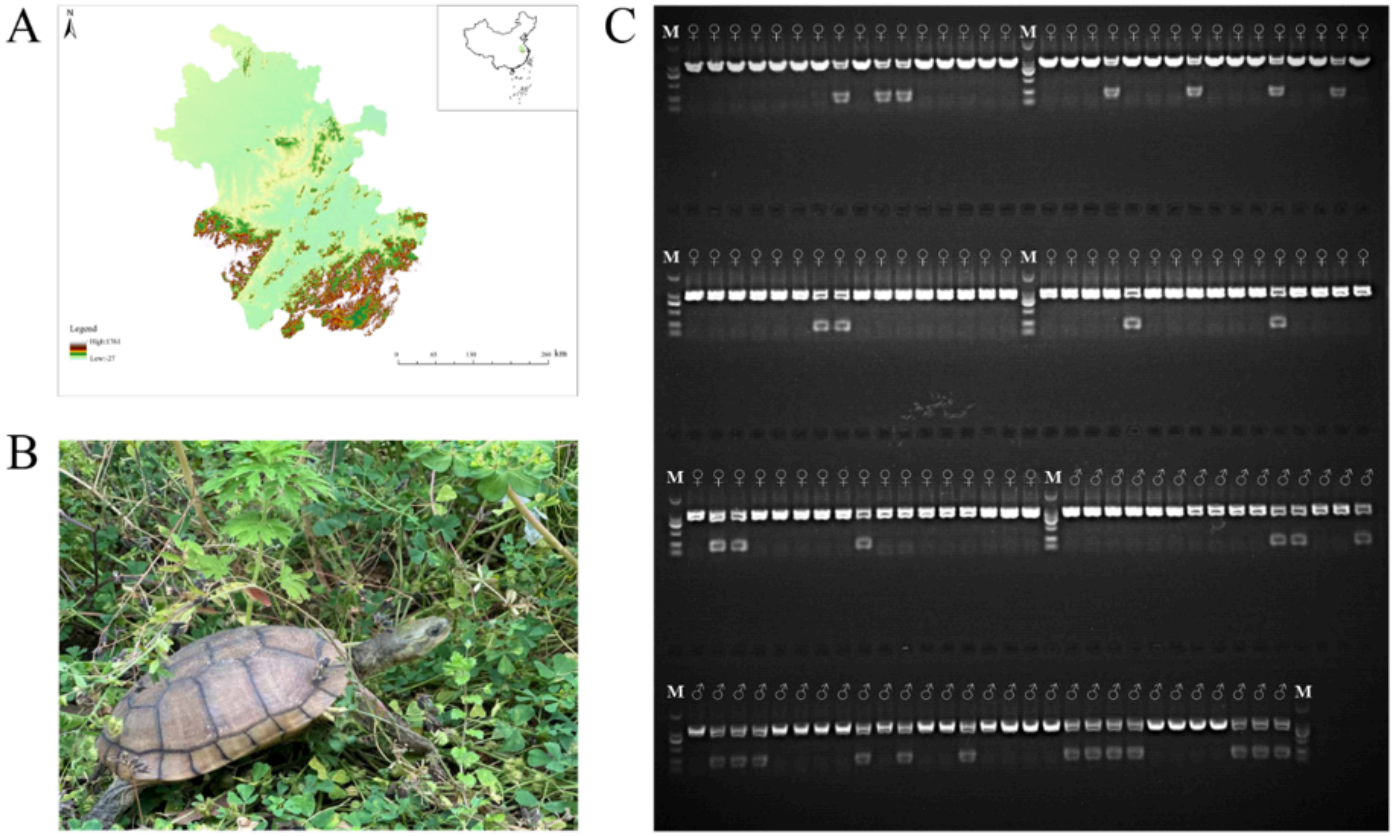


Figure 4

Molecular sex identification in natural *M. mutica*.

(A) Distribution of sampling sites in southern Anhui and the Lu'an region, Anhui Province, China. Sites are marked by colored dots (see Table 3 for coordinates). (B) A representative adult individual in its natural habitat. (C) PCR-based molecular sexing of natural adults. The mitochondrial *COX1* amplicon (1046 bp) served as an internal control and amplified successfully in all samples (top), whereas the Y-linked diagnostic fragment (223 bp) was detected only in a subset of individuals (bottom). The presence of the 223-bp band in some phenotypic females and its absence in some phenotypic males indicates

discordance between phenotypic and genotypic sex, consistent with sex reversal occurring under natural conditions.